

Planetary Gearbox Diagnosis Using Varying-stable Stochastic Resonance

Jianshe Kang, Kuo Chi*

Department of Equipment Command and Management
Army Engineering University of PLA
Shijiazhuang, China
*dynamicck@emails.imau.edu.cn

Qiongjie Tang

Combat Services Section, Support Department
Unit 75222
Chaozhou, China
68278427@qq.com

Xiaorong Jing

Maintenance and Support Center
Guilin, China

Zhiyong Li

Teaching and Training Department
Army Engineering University of PLA
Shijiazhuang, China

Fei Zhao

School of Business Administration
Northeastern University
Qinhuangdao, China

Abstract—Planetary gearbox is an important part of the mechanical devices, but the fault-induced impulses that induced by the fault and submerged in strong noise are too weak to be detected. Stochastic resonance (SR) can improve the weak signal with the help of noise, which suits the detection of the weak signal. Bi-stable SR (BSR) is the most classical SR and has been used for the mechanical fault diagnosis. Varying-stable SR (VSR), whose potential is the varying-stable potential, is proposed for the planetary gearbox diagnosis. Unlike the bi-stable potential, the number of varying-stable potential well is different under different parameters, which enhances the SR effect. To verify the proposed method, two planted fault tests of the planetary gearbox are carried out. For comparison, the fault signals are analyzed by BSR and VSR respectively. The results prove that VSR is feasible for the planetary gearbox diagnosis and more effective than BSR.

Keywords—Fault diagnosis; planetary gearbox; stochastic resonance; varying-stable potential

I. INTRODUCTION

Due to the compact size, big transmission ratio and impact resistance [1], planetary gearbox plays an important role in the transmission system of the mechanical devices such as helicopter [2], wind turbine [3] and nuclear reactor [4]. But because the operation environment is very bad and the dynamic load is very complex, the planetary gearbox often becomes fault, which results in the machine stops or even the accidents. For example, two helicopter crashes happened at Scotland in April 2009 and at Norway in June 2016, which are led by the fault of the planetary gearbox. Fig. 1 shows (a) the broken main rotor head and blades, (b) fault planet gears, and (c) fault



Figure 1. CHC airbus helicopters EC225 LN-OJF accident: (a) main rotor head and blades; (b) fault planet gears; (c) fault planet carrier and fault sun gear

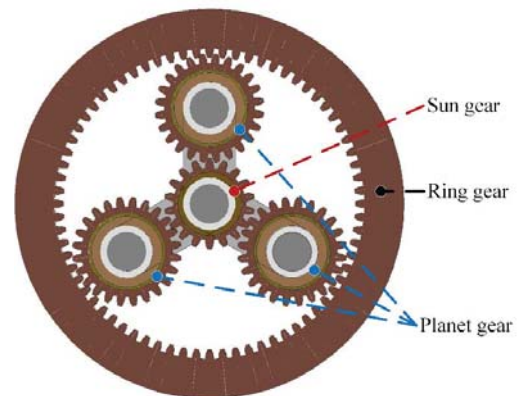


Figure 2. Diagram of a 3-planet planetary gear set

planet carrier with the fault sun gear of one of the two crashed helicopters. In a word, planetary gearbox diagnosis is extremely important for protecting the safety and property.

A 3-planet planetary gearbox structure is shown in Fig. 2, whose structure is more intricate than the fixed-axle gearbox. Unlike the fixed-axle gearbox, the planet gears of the planetary

gearbox rotate around both their own axis and sun gear axis. This special structure of planetary gearbox leads to the following characteristics: (1) the sun gear or the ring gear meshes with many planet gears concurrently, and many similar vibrations are excited. These similar vibrations that have different phases couple with each other, which may lead to vibration neutralization or elimination. (2) Multiple vibration transmission paths exist which can deteriorate and weaken the vibration signals due to the dissipation and interference-effect. (3) The weak impulses that caused by the fault are submerged in the strong noise due to the large transmission ratio [1]. Therefore, the planetary gearbox's vibration signal is complex and the impulses that caused by the fault are weak. Planetary gearbox diagnosis is difficult.

Most planetary gearbox methods are concerned on with the vibration signal under the invariable speed and the invariable load. Zhou, Duan, Corsar, Elasha and David [2] applied the self-adaptive noise cancellation, the kurtogram and the envelope analysis for the detection of the helicopter main gearbox fault. To diagnose the planetary gearbox of the wind turbine, Wang, Chu and Han [3] proposed a novel filtering algorithm via the meshing resonance phenomenon. Zhang, Kang, Xiao and Zhao [4] combined the alpha-stable distribution with the morphological filter for detection of the planetary gearbox fault. Li, Zhao, Song and Teng [5] combined the morphological filter with empirical mode decomposition for planetary gearbox diagnosis. However, further studies should be done because the vibration signals is too complexed and the impulses that caused by the fault are too weak.

Stochastic resonance (SR) is the phenomenon that the weak signal in a proper nonlinear system can be raised with the help of the proper noise. In other words, noise is helpful in some special cases rather than always harmful. In the early, the traditional SR is just used to process the low-frequency signal that lower than 1Hz. However, the mechanical fault characteristic frequency (FCF) is often bigger larger than 1Hz. To surmount this troublesome question, high-frequency SR methods are proposed like the step-changed SR [6] and the re-scaling SR [7]. In these methods, the high-frequency signal is changed into the low-frequency signal. With the emergence of the high-frequency SR methods, SR is used for the detection of the mechanical devices gradually. Lu, He and Wang [8] reviewed the SR application in rotating machinery. To detect the bearing fault, Chi, Kang, Zhang and Zhao [9] studied the scale-varying fractional-order SR.

However, most studies about SR focus on bi-stable SR (BSR), whose potential only has two wells. The potential with the fixed wells is not suitable for the extraction of the weak fault characters from the complex and diverse mechanical vibration signals. Unlike the bi-stable potential, the wells of the varying-stable potential are varying, which can enhance the SR effect. Thus, a novel SR based on varying-stable potential called VSR will propose for planetary gearbox diagnosis.

The rests are arranged as follows. In section II, introduce BSR will be introduced, VSR will be constructed, and then the planetary gearbox diagnosis strategy based on VSR will be proposed. In Section III, the planetary gearbox fault cases are

analyzed for the verification of the proposed method. In Section IV, the conclusion will be summarized.

II. VARYING-STABLE STOCHASTIC RESONANCE

Traditional SR can be described as:

$$\frac{dx}{dt} = -\frac{dU(x)}{dx} + S(t) + \Gamma(t), \quad (1)$$

where x is the motion trajectory of the particle. $U(x)$ is the potential. $S(t)=A_0\sin(2\pi f_d t)$ is the driving signal that whose amplitude is A_0 and frequency is f_d . $\Gamma(t)=\sqrt{2D}\varepsilon(t)$ is Gaussian white noise (GWN) with the intensity D . $\varepsilon(t)$ is the standard GWN.

A. Bi-stable stochastic resonance

The most classical SR is the bi-stable SR (BSR), whose potential is the bi-stable potential $U_B(x)$:

$$U_B(t) = -\frac{a^2}{2}x^2 + \frac{b^4}{4}x^4, \quad (2)$$

where $a \in \mathcal{R}^+$ and $b \in \mathcal{R}^+$. Fig. 3 is the shape of bi-stable potential. From Fig. 3, we can find that the $U_B(x)$ has two minimas at $(\pm x_m, -\Delta U)=(\pm \sqrt{a/b}, a^2/4b)$ called potential well and a maximum at $(0, 0)$ called potential barrier. Thus, Eq. (1) becomes:

$$\frac{dx}{dt} = ax - bx^3 + S(t) + \Gamma(t). \quad (3)$$

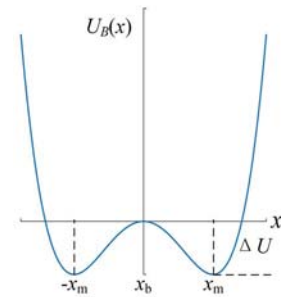


Figure 3. The shape of bi-stable potential

When the signal is discrete, Eq. (3) can be calculated by the Runge-Kutta method [8]. If the driving signal amplitude and the driving frequency is small, the BSR output can be obtained as [10]:

$$\begin{cases} \langle x(t) \rangle = \bar{x} \sin(2\pi f_d - \bar{\phi}), \bar{x} = \frac{A_0 \langle x^2 \rangle_0}{D \sqrt{r_k^2 + \pi^2 f_d^2}}, \\ r_k = \frac{a}{\sqrt{2\pi}} \exp\left(-\frac{a^2}{4bD}\right), \bar{\phi} = \arctan(\pi f_d / r_k) \end{cases} \quad (4)$$

where $\langle x(t) \rangle$ is the BSR output. \bar{x} is the amplitude of BSR output. $\bar{\phi}$ is the phase lag. $\langle x^2 \rangle_0$ is the variance of the stationary unperturbed system ($A_0=0$) that be dependent on noise intensity D . r_K is the Kramers rate.

B. Varying-stable stochastic resonance

1) Varying-stable stochastic resonance

The varying-stable potential is as:

$$U_v(x) = -\frac{a}{2}(|x|-c)^2 + \frac{b}{4}(|x|-c)^4, \quad (5)$$

where $c \in (-\infty, \sqrt{a/b}]$ is the potential parameter, which matters the number of the wells.

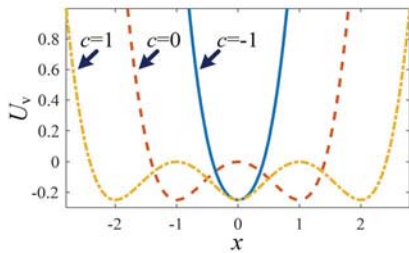


Figure 4. Shapes of the vary-stable potential with $a=1$, $b=1$ and $c \in [-1, 0, 1]$

The number of potential wells is different under different parameter c . When $c \in (-\infty, -\sqrt{a/b}]$, potential $U_v(x)$ only has a well. When $c \in [-\sqrt{a/b}, 0]$, it has two wells. When $c \in [0, \sqrt{a/b}]$, three wells. Fig. 4 shows the shapes of potential $U_v(x)$ when $a=1$, $b=1$ and $c \in [-1, 0, 1]$. From Fig. 4, we can find that the well number of the potential $U_v(x)$ increases with the increment of parameter c .

Because $U_v(0)$ does not exist, we assume that $U_v(0)=0$ for subsequent calculations. Substituting Eq. (5) into Eq. (1), the LE of varying-stable SR (VSR) is:

$$\frac{dx}{dt} = \text{sgn}(x) \left(a(|x|-c) - b(|x|-c)^3 \right) + S(t) + \Gamma(t), \quad (6)$$

where

$$\text{sgn}(x) = \begin{cases} -1, & \text{if } x < 0 \\ 0, & \text{if } x = 0 \\ 1, & \text{if } x > 0 \end{cases}. \quad (7)$$

Let $z = \sqrt{b/a}x$ and $\tau = at$, Eq. (6) is transformed into

$$\begin{aligned} \frac{dz}{dt} &= \text{sgn}(z) \left(\left(|z| - c\sqrt{\frac{b}{a}} \right) - \left(|z| - c\sqrt{\frac{b}{a}} \right)^3 \right) + K \left[S\left(\frac{\tau}{a}\right) + \Gamma\left(\frac{\tau}{a}\right) \right] \\ &= -\frac{d \left(\frac{1}{2} \left(|z| - c\sqrt{\frac{b}{a}} \right)^2 - \frac{1}{4} \left(|z| - c\sqrt{\frac{b}{a}} \right)^3 \right)}{dx} + K \left[S\left(\frac{\tau}{a}\right) + \Gamma\left(\frac{\tau}{a}\right) \right], \quad (8) \\ &= -\frac{d \left(\frac{1}{2} (|z|-C)^2 - \frac{1}{4} (|z|-C)^3 \right)}{dx} + K \left[S\left(\frac{\tau}{a}\right) + \Gamma\left(\frac{\tau}{a}\right) \right] \end{aligned}$$

where $C = c\sqrt{b/a} \in (-\infty, 1]$ and $K = \sqrt{b/a}$. After transformation, both of parameter a and b become 1. The driving frequency f_d becomes $1/a$ times of the original driving frequency. Through the transformation, the high-frequency signal is changed into a low-frequency signal, which satisfies the low-frequency limitation of the traditional SR.

2) Implement of VSR for discrete signal

In engineering, the signal is always discrete. For the discrete signal, the Runge-Kutta method is used to solve Eq. (8) as:

$$\begin{cases} f(n, z|C, H, K, s) = \text{sgn}(z) \left[(|z|-C) - (|z|-C)^3 \right] + s \\ z_{n+1} = z_n + \frac{H}{6} (k_1 + k_2 + 2k_3 + k_4 + k_5) \\ k_1 = f(n, z_n|C, H, K, s_n) \\ k_2 = f\left(n, z_n + \frac{H}{2}k_1|C, H, K, s_n\right) \\ k_3 = f\left(n+1, z_n + \frac{H}{2}k_2|C, H, K, s_{n+1}\right) \\ k_4 = f\left(n+1, z_n + \frac{H}{2}k_3|C, H, K, s_{n+1}\right) \\ k_5 = f(n+1, z_n + Hk_4|C, H, K, s_{n+1}) \end{cases}, \quad (9)$$

where $z_1=0$. H is the integral step. $s=S+\Gamma$ is the collected signal that is the mixture of driving signal and noise. s_n and z_n are the n -th point of the collected signal and the VSR output respectively.

3) Evaluation of VSR output

Because of the simple calculation and clear definition, signal-to-noise ratio (SNR) is used for the evaluation of the VSR output z . It is defined as:

$$\text{SNR} = 10 \log \left(\frac{A_d}{A_n} \right), \quad (10)$$

where A_d is the driving signal power and A_n is the noise power.

arger the SNR is, better the VSR output z is. According to this idea, an objective function for searching the best parameters (C, H, K) is modeled as:

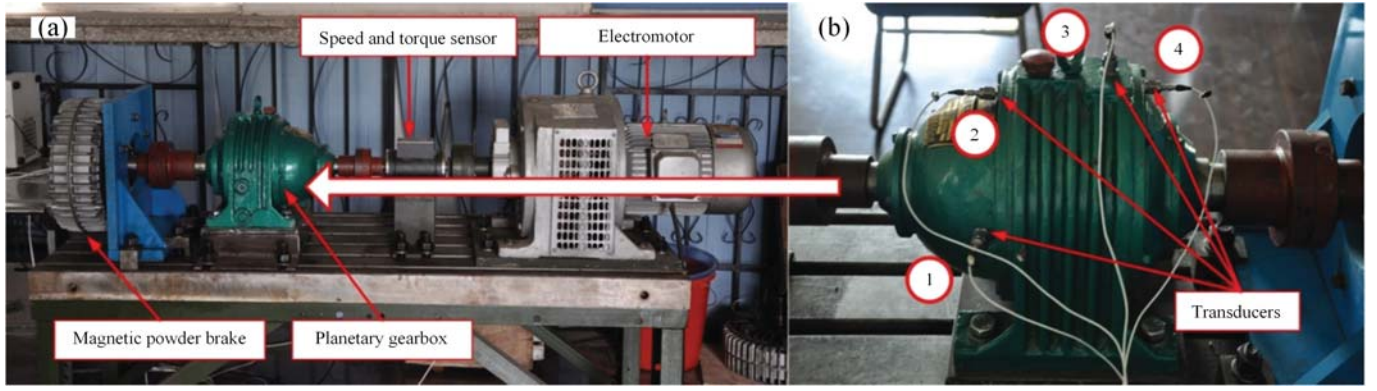


Figure 5 (a) Planetary gearbox fault test rig and (b) the four transducer locations

$$(C, H, K) = \arg \max [\text{SNR}(z)] \quad (11)$$

C. Fault diagnosis strategy based on VSR

The planetary gearbox diagnosis strategy based on VSR according to Eq. (11) is as follows:

1) *Signal preprocessing*. Some common techniques are applied to processing the vibration signal, including filtering out the noises, envelope demodulation, and spectral editing. Then, the preprocessed signal is obtained.

2) *Initialization of the parameters*. The search ranges of parameters (C, H, K) and their initial values are set.

3) *Calculation of VSR output*. The VSR output is calculated according to Eq. (9).

4) *Evaluation of VSR output*. SNR is calculated according to Eq. (10). If SNR reaches the max, go on the next step. Otherwise, change the parameters (C, H, K) and jump to step 3.

5) *Analysis and diagnosis*. The max SNR, optimal parameter and best VSR output are recorded. Best VSR output is analyzed by the spectrum analysis. The planetary gearbox is diagnosed.

III. VERIFICATION

A. Experiment

Two pre-planting fault tests of the planetary gearbox are carried by the test rig as shown in Fig. 5(a). Four transducers are set to collect the vibration signal, whose locations are shown in Fig. 5(b). The planetary gearbox is single-stage and its type is NGW-11, whose structure and main parameters are shown in Fig. 2 and Table I. Fig. 6 shows the pre-planted wear faults of sun gear and ring gear respectively. The parameter of the two tests are set as follows: sample frequency $f_s=5000\text{Hz}$, signal length $N=3 \times 10^4$ and rotate speed of the motor $n_1=20 \text{ r/s}$. Because the energy of the signal from transducer 3 is the max, we just analyze the signal from transducer 3. Table II shows the calculation formulars for the planetary gearbox FCFs. According to motor rotate speed n_1 , planetary gearbox main parameters (Table I) and FCF calculation formulars (Table II), the relevant frequencies are obtained shown in Table III.

TABLE I. MAIN PARAMETERS OF THE PLANETARY GEARBOX

| | Sun gear Z_s | Gear ring Z_R | Planet gear Z_p |
|-------------------------|----------------|-----------------|-------------------|
| Teeth (Num. of gear) | 13 (1) | 146 (1) | 64 (3) |

TABLE II. CALCULATION FORMULAS OF MAIN FREQUENCIES AND FCFs OF THE PLANETARY GEARBOX

| Names | Formulas |
|-----------------------------|--|
| Transmission ratio | $i_{12} = Z_R / Z_s + 1$ |
| Planet carrier rotate speed | $f_c = n_1 / i_{12}$ |
| Gear meshing frequency | $f_m = f_c Z_R$ |
| Sun gear FCF | $f_s = N f_m / Z_s$ |
| Ring gear FCF | $f_R = N f_m / Z_R$ |
| Planet gear FCF | $f_{p1} = f_m / Z_p, f_{p2} = f_m / Z_p$ |

Note: N is the planet gears number. n_1 is the rotate speed of the sun gear. FCF means the fault characteristic frequency.

TABLE III. RELEVANT PLANETARY GEARBOX CHARACTERISTIC FREQUENCIES

| n_1 | f_c | f_m | f_s | f_R | f_{p1} | f_{p2} |
|-------|-------|---------|--------|-------|----------|----------|
| 20 | 1.635 | 238.742 | 55.094 | 4.905 | 3.730 | 7.460 |

Unit: Hz

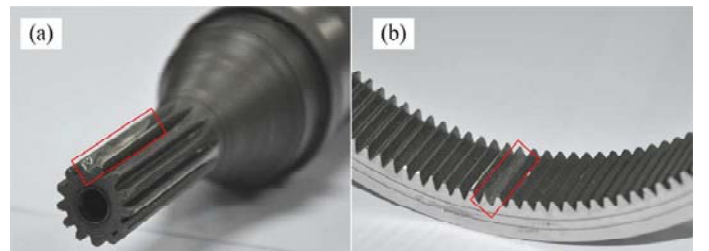


Figure 6. Pre-planted faults: (a) the sun gear and (b) the ring gear.

B. Fault case of the sun gear

Firstly, the fault signal of the sun gear is analyzed. The low-frequency components that lower than 1kHz are filtered by the 10-order Butterworth filter. Then, the envelope signal is got through Hilbert transform. DC component is also eliminated. Fig. 7(a) shows the preprocessed signal. After signal preprocessing, the sun gear FCF f_s is enhanced. Then, BSR and VSR are used to enhance the preprocessed signal respectively. Fig. 7(b) and (c) show BSR output and VSR output. After SR,

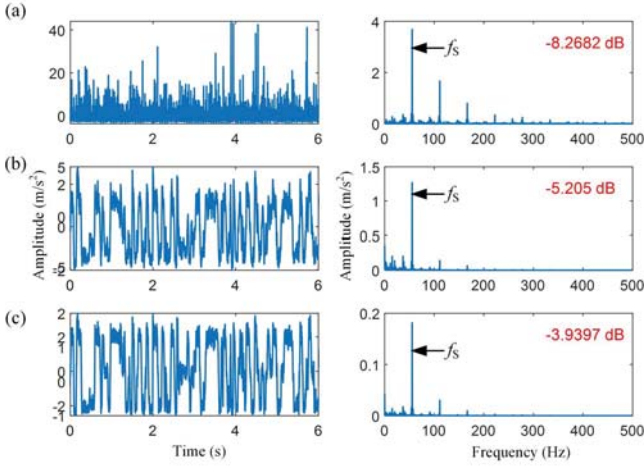


Figure 7. Analyzed results of the sun gear fault signal: (a) Preprocessed signal; (b) BSR output with $(H, K)=(0.0894, 1.1000)$; (c) VSR output with $(C, H, K)=(0.242, 0.614, 0.0599)$

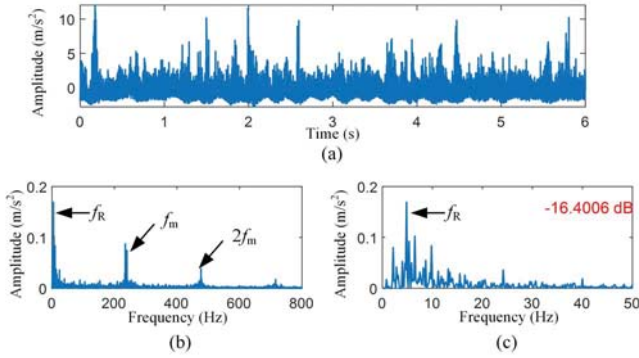


Figure 8. Preprocessed result of the gear ring fault signal: (a) Waveform; (b) Spectrum in $[0, 800]$ Hz; (c) Spectrum in $[0, 50]$ Hz.

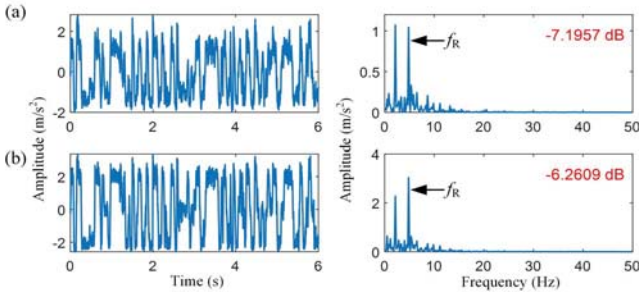


Figure 9. Analyzed results of the ring gear fault signal: (a) BSR output with $(H, K)=(0.0091, 3.7115)$; (b) VSR output with $(C, H, K)=(1, 1.162, 0.0431)$

the FCF f_s is enhanced and the high frequencies are suppressed. The SNR of VSR output is larger than BSR, which means that VSR is more effective than BSR.

C. Fault case of the ring gear

Subsequently, the fault signal of gear ring is analyzed. The low-frequency components that lower than 1kHz are filtered by the 10-order Butterworth filter. Envelope signal is got through Hilbert transform. DC component and rotating frequency f_c are eliminated. Fig. 8 shows the preprocessed signal. The gear meshing frequency f_m is the main component as shown in Fig.

8(b). The low-frequency areas are shown in Fig. 8(c). The gear ring FCF f_R can be found. The preprocessed signal is inputted to the BSR and VSR respectively. Then, BSR and VSR are used to enhance the preprocessed signal. Their SR outputs are obtained as shown in Fig. 9(a) and (b). The high-frequency components like the frequency f_m are removed. Both output SNRs are enhanced. Moreover, the SNR of the VSR output is also larger than BSR. Thus, VSR can enhance the gear ring FCF f_R better than BSR. But some low-frequency components that lower than f_R are also enhanced. Therefore, BSR and VSR cannot suppress the low-frequency components that lower than the driving frequency.

IV. CONCLUSIONS

To diagnose the weak fault of the planetary gearbox, varying-stable stochastic resonance (VSR) is proposed. Unlike the bi-stable potential, the number of the varying-stable potential well is tuned by the potential parameter C , which is suitable for extraction of the weak fault impulses from the complex and diverse mechanical vibration signal. Sun gear pre-planted fault test and gear ring pre-planted fault test are carried out. For comparison, both BSR and VSR are applied to the detection of fault signals. The results show that:

- (1) VSR is feasible for the planetary gearbox diagnosis because of the new varying-stable potential whose well number is varying;
- (2) VSR can enhance the weak fault-induced impulses more effectively than BSR because the SNR of VSR output is always higher than the SNR of BSR output;
- (3) Similar to BSR, VSR also enhances the low-frequency components and remove the high-frequency components, which is like a lowpass filter.

REFERENCES

- [1] Y. Lei, J. Lin, M. Zuo, and Z. He, "Condition monitoring and fault diagnosis of planetary gearboxes: A review," *Measurement*, vol. 48, pp. 292-305, February 2014.
- [2] L. Zhou, F. Duan, M. Corsar, F. Elasha, and M. David, "A study on helicopter main gearbox planetary bearing fault diagnosis," *Applied Acoustics*, vol. 147, pp. 4-14, 2017.
- [3] T. Wang, F. Chu, and Q. Han, "Fault diagnosis for wind turbine planetary ring gear via a meshing resonance based filtering algorithm," *ISA Transactions*, vol. 67, pp. 173-182, 2017.
- [4] X. Zhang, J. Kang, L. Xiao, and J. Zhao, "Alpha Stable Distribution Based Morphological Filter for Bearing and Gear Fault Diagnosis in Nuclear Power Plant," *Science and Technology of Nuclear Installations*, vol. 2015, pp. 1-15, November 2015.
- [5] H. Li, J. Zhao, W. Song, and H. Teng, "An offline fault diagnosis method for planetary gearbox based on empirical mode decomposition and adaptive multi-scale morphological gradient filter," *Journal of Vibroengineering*, vol. 17, no. 2, pp. 705-719, April 2015.
- [6] Z. Zhang, D. Wang, T. Wang, J. Lin, and Y. Jiang, "Self-adaptive step-changed stochastic resonance using particle swarm optimization," *Journal of Vibration and Shock*, vol. 32, no. 19, pp. 125-130, 2013.
- [7] J. Liu, Y. Leng, S. Fan, and X. Ma, "An Improved Re-Scaling Frequency Stochastic Resonance and its Application to Weak Fault Signal Detection," in *Proceedings of the ASME 2017 International Design Engineering Technical Conferences and Computers and Information in Engineering Conference*, Cleveland, 2017, pp. 1-6.

- [8] S. Lu, Q. He, and J. Wang, "A review of stochastic resonance in rotating machine fault detection," *Mechanical Systems and Signal Processing*, vol. 116, pp. 230-260, February 2019.
- [9] K. Chi, J. Kang, X. Zhang, and F. Zhao, "Effect of scale-varying fractional-order stochastic resonance by simulation and its application in bearing diagnosis," *International Journal of Modeling, Simulation, and Scientific Computing*, vol. 10, no. 1, pp. 1-21, February 2019.
- [10] L. Gamaitoni, P. Hänggi, P. Jung, and F. Marchesoni, "Stochastic resonance," *Review of Modern Physics*, vol. 70, no. 1, pp. 223-287, January 1998.